# SEISMIC PERFORMANCE OF MULTI-SPAN RC RAILWAY BRIDGES

**C.T. Georgakis[1] and X. Barrau[2]**

[1] *Associate Professor, Dept. of Civil Engineering, Technical University of Denmark, Copenhagen, Denmark*
[2] *Junior Engineer, PEDELTA Consulting Engineers, Barcelona, Spain*
*Email: cg@byg.dtu.dk, xavier.barrau@gmail.com*

**ABSTRACT:**
Presently, there is no clear method for determining the optimal railway bridge design for a particular ground type and expected seismic intensity. Four main types of RC bridge dominate the current multi-span railway bridge design trends – the Simply Supported Beam, Continuous Box-Girder (CBG), CBG with Lead Rubber Bearing (LRB) supports and the laterally fixed continuous deck (CRB) with LRBs. In this paper, the seismic performance of these four types is examined for varying ground types and seismic intensities. For the purposes of comparison, all of the bridges have five spans with identical span lengths and topography. Initially, typical bridge deck, pier and bearing configurations are chosen and analyzed through a series of nonlinear time-history analyses using synthetic accelerograms, in which plastic hinge formation is permitted. Next, an optimization of the bridge configurations is undertaken to increase the performance and reduce the overall bridge cost. Finally, an evaluation of the lifetime bridge costs are made assuming current prices, including costs relating to the damage associated with the expected seismic events. This is accomplished through the use of approximated damage states and fragility curves in relation to PGA. The cost comparisons clearly show that particular bridge types perform better than others economically for specific ground types and expected seismic intensities, even though in some cases they may be expected to suffer larger damages during their lifetime.

**KEYWORDS:** RC bridge design, seismic performance, design-life costs

## 1. INTRODUCTION

During the design of a bridge, the decision on the structural configuration that should be used is of primary importance. This decision should be based on a number of factors that, in a seismic zone, may be dominated by the expected earthquake intensity and soil conditions. The chosen configuration will not only determine the performance of the bridge, but also the overall design-life costs.

Different bridge configurations will result in different construction and design-life maintenance costs, whilst the allowance of limited damage during a seismic event might lead to significant repair costs. As a consequence, the question of which bridge configurations are optimal for particular site conditions immediately arises. Since one of the primary goals of the design process is to achieve expected bridge functionality with the lowest cost, it is of interest to determine the bridge configuration that is most cost-effective over its entire design-life.

In this paper, a methodology is presented, in which the design-life costs of bridge can be determined for any soil condition and expected earthquake intensity. More specifically, three reinforced concrete (RC) box-girder bridges of varying configurations are evaluated through a parametric study for their design-life costs, assuming different soil conditions and earthquake intensities. Comparisons are made based on estimates of current costs. The comparisons clearly show significant differences in design-life bridge costs from one bridge configuration to another.

## 2. EXAMPLE BRIDGE

The presentation of the methodology is initiated with the selection of a generic example bridge. The selected

bridge is a five-span RC railway bridge with a total length of 207 m and 13 m deck width. The three central spans are 45-meter long, with two side spans 36-meter in length. The bridge has four piers with uneven heights; two central piers of 25 m and two end piers of 15 m in height, Fig.1.

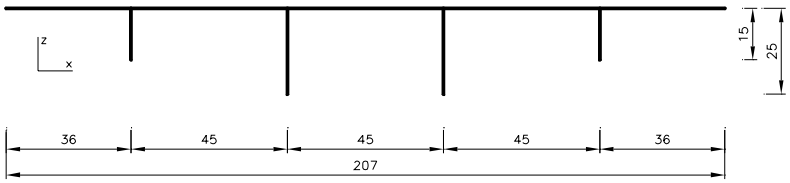


Figure 1 Elevation of generic example bridge

### 2.1. Bridge configurations

Four different bridge configurations are chosen for comparison. They are namely, the Simply Supported Bridge (SSB), the Continuous Box-Girder (CBG), the Continuous Box-Girder with Lead Rubber Bearings (LRB) and the laterally fixed continuous deck with lead rubber bearings (CRB), Fig. 2a,b and c.

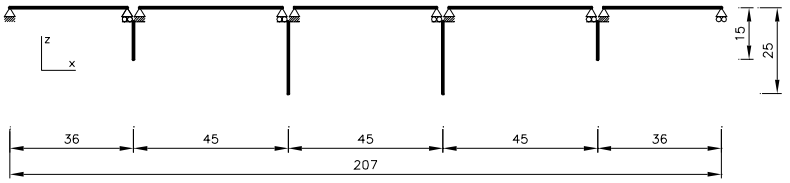


Figure 2a Simply Supported Bridge (SSB)

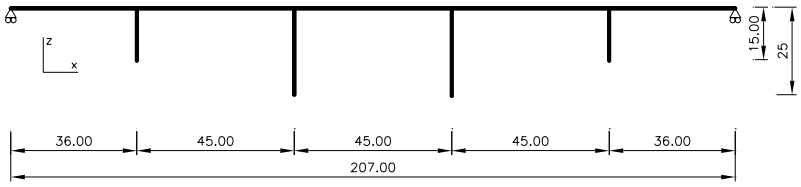


Figure 2b Continuous Box Girder (CBG)

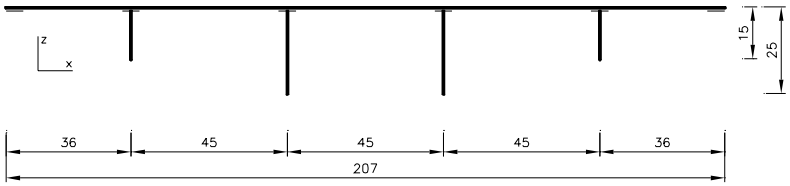


Figure 2c Continuous Box-Girder with Lead Rubber Bearing (LRB) and (CRB)

The SSB's deck is comprised of six simply-supported (at the piers) I-beams across with lateral fixation. The CBG has a continuous box-girder monolithically joined to piers. The deck is free to move in longitudinal direction at abutments. The LRB is similar to the CBG, but isolated from the piers and abutments by lead rubber bearings that allow movement in both longitudinal and lateral directions. Finally, the CRB has a laterally fixed continuous deck with lead rubber bearing supports. All of the piers have rectangular hollow pier sections.

### 2.2. Expected bridge behaviour and design strategy

For all of the bridges, the deck is expected to remain undamaged after a major seismic event since it is the element that affords the functionality to the bridge. Plastic hinges are expected to form in the piers of the SSB and CBG configurations. In contrast, the piers of the LRB and CRB configurations, endowed with lead rubber bearings, are not expected to form plastic hinges given that the lead rubber bearings have the necessary capacity

to dissipate a large proportion of the seismic energy.

The first two bridge configurations may be classified as "in-elastic", whilst the remaining two as "elastic". From an economic perspective, these two classifications result in widely varying construction and design-life costs. Whilst the structural members of the SSB and CBG configurations will be dimensioned to resist the full seismic loading and will have to be repaired after a major seismic event, the structural members of the LRB and CRB bridges will be dimensioned with reduced seismic loading and will be subject to significantly reduced repair costs after such an event. Nevertheless, the preliminary and design-life maintenance costs for the lead rubber bearings on the LRB and CRB bridges are significant.

## 3. PARAMETRIC STUDY

A parametric study of the example railway bridge is undertaken. Three seismic intensities are represented by three base accelerations –0.16g, 0.24g and 0.36g– and three ground types –A, C and E–, following Eurocode 8 (1998). Results from only three of the four bridge configurations are presented, as the CRB was found to be the most expensive solution in all cases. The combination of these parameters results in a matrix of nine case combinations per bridge configuration.

## 4. MODEL OF THE BRIDGE AND ANALYSIS

The parametric study is performed through the finite element (FE) modelling and analysis of the bridges. The FE modelling of the bridge was undertaken using SOLVIA03 (2006). For the modelling of both the deck and piers, multiple linear-elastic beam elements were used in all locations, except for those in which plastic hinge formation was expected. For the modelling of the plastic hinges, bi-linear hysteretic (kinematic-hardening) spring elements, with ultimate capacity fuses, were employed, following Georgakis & MacKenzie (2002). The bi-linear spring element moment/rotation properties were based on the yield moment/rotation and ultimate moment/rotation of the pier at the plastic hinge location. As such, both yield moment/rotation and ultimate moment/rotation had to be calculated for each plastic hinge location, on every pier in both longitudinal and transverse directions.

The yield moment, $M_y$, was calculated as:

$$M_y = \varphi_y E_c I_c \tag{4.1}$$

where: $E_c$ is the concrete modulus of elasticity and $\varphi_y = 0.004/d$ (where $d$ is the effective depth of the section). The cracked moment of inertia $I_c$ is found assuming a ratio between initial and cracked moments of inertia,

$$\frac{I_c}{I_i} = 0.45 \tag{4.2}$$

where: $I_i$ is the initial member moment of inertia. The ultimate moment, $M_u$, is assumed to be $M_u = 1.1\ M_y$.

Plastic hinge yielding and ultimate rotations were calculated as:

$$\theta_y = \varphi_y L_p \tag{4.3}$$

$$\theta_u = \varphi_u L_p \tag{4.4}$$

where: the plastic hinge length, $L_p$, was calculated as:

$$L_p = 0.08\,H + 0.022\,f_{ye}\,d_{bl} \tag{4.5}$$

where: $H$ is the pier height, $f_{ye}$ is the yield stress of longitudinal reinforcement and $d_{bl}$ is the diameter of longitudinal reinforcement (in meters). The ultimate member curvature is found as,

$$\varphi_u = \frac{\varepsilon_{cu}}{d/2} \tag{4.6}$$

The ultimate concrete strength, $\varepsilon_{cu}$, will be:

$$\varepsilon_{cu} = 0.004 + \frac{1.4\,\rho_s\,f_{yh}\,\varepsilon_{su}}{f_{cu}} \tag{4.7}$$

where: $\rho_s$ is the transverse steel volumetric ratio, $f_{yh}$ is the yield stress of transverse reinforcement, $\varepsilon_{su}$ is ultimate steel strain and $f_{cu}$ is the concrete ultimate stress. According to [2], $f_{cu}$ is,

$$f_{cu} = f_c^{'}\left(2.254 + \sqrt{1 + 7.94\frac{f_l^{'}}{f_c^{'}}} - 2\frac{f_l^{'}}{f_c^{'}} - 1.254\right) \tag{4.8}$$

and the effective lateral confining stress, $f_l^{'}$, is:

$$f_l^{'} = 0.6\,\rho_x\,f_{yh} \tag{4.9}$$

Yielding member curvature is calculated assuming a curvature ductility $\mu_\varphi = 18$, so that:

$$\varphi_y = \frac{\varphi_u}{\mu_\varphi} = \frac{\varphi_u}{18} \tag{4.10}$$

Expressions 3.1 to 3.10 lead to the yielding and ultimate moments and rotations for the definition of the bi-linear hysteretic plastic hinge models.

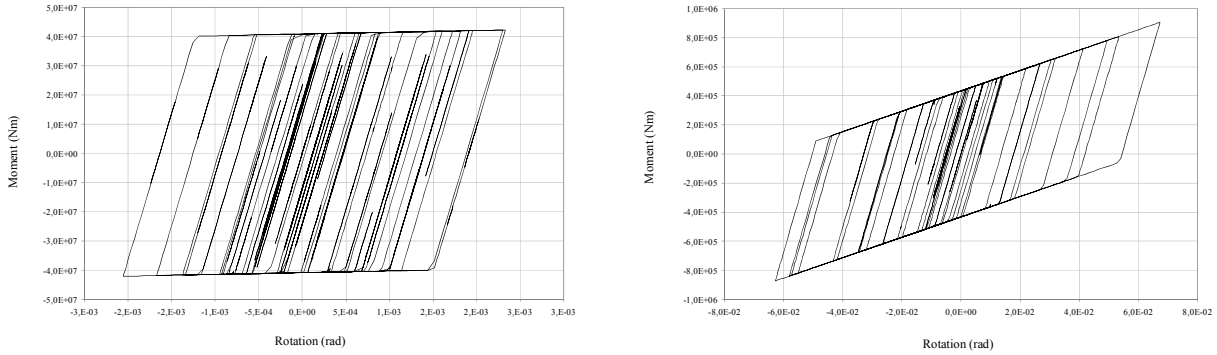


Figure 4 Example moment/rot diagrams of a pier plastic hinge (left) and a lead rubber bearing (right)

*4.1.1. Lead rubber bearing model*

For the lead rubber bearings, a bi-linear force-displacement relationship is employed. The linear relationship between force and displacement before yielding is determined by the rubber shear stiffness, $K_r$, where:

$$K_r = \frac{G_r A_r}{h} \tag{4.11}$$

The horizontal force required for shear yielding of the bearing can be found as the addition of the force due to lead plasticity and the rubber elasticity, so that:

$$F_h = \tau_{Pb} A_{Pb} + K_r x \tag{4.12}$$

where: $\tau_{Pb}$ is the lead yield shear stress, $A_{Pb}$ is the cross-section area of lead and $x$ is the displacement of the top surface of the bearing. The allowable maximum displacement is:

$$\Delta_{\max} = B\left(1 - \frac{A'}{A}\right) \tag{4.13}$$

where: $B$ is the side dimension of the bearing in the considered direction, and $A'$ is the overlap area between top and bottom bearing surfaces.

The vertical stiffness of the support is:

$$K_z = \frac{6 G_r S^2 A_r \kappa}{\left(6 G_r S^2 + \kappa\right) h} \tag{4.14}$$

where: $S$ is the bearing shape factor, taken as 18 here, and $\kappa$ is the rubber compression modulus.

Finally, the vertical load capacity of the bearing is:

$$W_{\max} = A' G_r S \gamma_{xz} \tag{4.15}$$

where: $\gamma_{xz}$ is the allowable rubber shear strain.

### 4.2. Structural damping

The structural damping of the bridges is modelled using mass-proportional Rayleigh damping, so that the damping for the n$^{th}$ vibration mode $\zeta_n = \alpha / 2\omega_n$. The equivalent damping ratio for the first modes of vibration is chosen to be 1% for all the bridges.

## 5. DYNAMIC ANALYSIS

The dynamic analysis is performed by means of a non-linear time-history analysis based on synthetic accelerograms, following Georgakis & MacKenzie (2002). The accelerograms are created using random seeds so as to be compatible with the response spectra, as defined by Eurocode 8. The choice of three different ground types and the three base accelerations for the parametric study lead to nine individual response spectra that are used to create twenty-seven unique synthetic accelerograms for each bridge configuration. As a result, 108 time-histories were performed.

## 6. OPTIMIZATION PROCESS

During the parametric study, a bridge optimization is undertaken using the traditional force-based design philosophy. Stresses at piers and deck as well as moments at plastic hinges and forces in the lead rubber bearings are checked after each iteration, as are reactions at pier foundations and abutments. In order to ensure

that the deck remains undamaged during the seismic event, a capacity-protected design philosophy is applied in the optimization process for this specific member. This is achieved by applying an additional safety factor for stress of 1.3. Piers are dimensioned with a reduction of 1.5 on the concrete material safety factor. Plastic hinges, however, are designed with characteristic material strengths.

The optimization process employed for the SSB and CBG configurations significantly differs to that used for the LRB configuration, due to the allowance of the plastic hinge formations in the former. For the SSB and CBG configurations, two criteria are used when dimensioning the sections: non-exceedance of the reduced concrete strength in elastic members and non-exceedance of the ultimate moment in members with plastic hinges. To fulfil these requirements, the section depth and wall thickness of the rectangular hollow sections are adjusted accordingly. For the LRB configuration, in which piers are expected to remain elastic, the criteria for pier dimensioning is for the reduced concrete strength and the yielding moment of the sections not to be exceeded.

### 6.1 Resulting member dimensions

Table 6.1 shows the member dimensions resulting from the optimization process. The numerical value represents the section depth in mm, whilst BG signifies Box Girder.

Table 6.1 Deck dimensions in mm

| Case | SSB | CBG | LRB |
|---|---|---|---|
| **Low A** | 6 I-Beams 2500 | BG 1675 | BG 1500 |
| **Low B** | 6 I-Beams 4100 | BG 1800 | BG 1500 |
| **Low C** | 6 I-Beams 4390 | BG 1825 | BG 1550 |
| **Medium A** | 6 I-Beams 3300 | BG 1850 | BG 1600 |
| **Medium B** | 6 I-Beams 5275 | BG 1900 | BG 1600 |
| **Medium C** | 6 I-Beams 5325 | BG 2100 | BG 1650 |
| **High A** | 6 I-Beams 5325 | BG 2250 | BG 1950 |
| **High B** | 6 I-Beams 5600 | BG 2375 | BG 2100 |
| **High C** | 6 I-Beams 7100 | BG 2850 | BG 2100 |

Table 6.2 shows the pier dimensions resulting from the same optimization process. The first dimension in each cell corresponds to the short piers (15 m in height), whilst the second corresponds to the long piers (25 m). It is important to note that the wall thickness decreases from 0.35m at the bottom to 0.25m at the top in all the cases. As such, the noted dimensions in the table correspond to the bottom section of piers.

Table 6.2 Short pier, long pier and lead rubber bearing dimensions (m)

| Case | **SSB**<br>L x W x Thickness | **CBG**<br>L x W x Thickness | **LRB**<br>L x W x Thickness | **Lead Rubber Bearings** |
|---|---|---|---|---|
| **Low A** | 3.55 x 1.30 x 0.35<br>3.55 x 1.30 x 0.35 | 3.00 x 1.20 x 0.35<br>3.00 x 1.20 x 0.35 | 3.35 x 1.25 x 0.35<br>3.35 x 1.25 x 0.35 | 5.60 x 5.60 x .85 |
| **Low B** | 4.00 x 1.45 x 0.35<br>4.00 x 1.45 x 0.35 | 3.15 x 1.40 x 0.35<br>3.15 x 1.40 x 0.35 | 3.80 x 1.30 x 0.35<br>3.80 x 1.30 x 0.35 | 5.60 x 5.60 x .85 |
| **Low C** | 4.35 x 1.60 x 0.35<br>4.35 x 1.60 x 0.35 | 3.40 x 1.45 x 0.35<br>3.40 x 1.45 x 0.35 | 3.80 x 1.40 x 0.35<br>3.80 x 1.40 x 0.35 | 5.80 x 5.80 x .90 |
| **Medium A** | 4.10 x 1.45 x 0.35<br>4.10 x 1.45 x 0.35 | 3.15 x 1.40 x 0.35<br>3.15 x 1.40 x 0.35 | 3.30 x 1.25 x 0.35<br>3.30 x 1.25 x 0.35 | 5.90 x 5.90 x .90 |
| **Medium B** | 5.70 x 2.10 x 0.35<br>5.70 x 2.10 x 0.35 | 3.40 x 1.50 x 0.35<br>3.40 x 1.50 x 0.35 | 3.80 x 1.75 x 0.35<br>3.80 x 1.75 x 0.35 | 5.90 x 5.90 x .90 |
| **Medium C** | 6.15 x 2.20 x 0.35<br>6.15 x 2.20 x 0.35 | 3.60 x 1.75 x 0.35<br>3.60 x 1.75 x 0.35 | 3.80 x 1.75 x 0.35<br>3.80 x 1.75 x 0.35 | 5.90 x 5.90 x .90 |
| **High A** | 6.50 x 3.25 x 0.35<br>6.80 x 3.30 x 0.35 | 3.45 x 1.45 x 0.35<br>3.45 x 1.45 x 0.35 | 4.30 x 2.10 x 0.35<br>4.30 x 2.10 x 0.35 | 6.40 x 6.40 x 1.00 |
| **High B** | 7.00 x 3.60 x 0.35<br>8.00 x 4.00 x 0.35 | 3.70 x 1.50 x 0.35<br>3.70 x 1.80 x 0.35 | 5.70 x 2.30 x 0.35<br>5.70 x 2.30 x 0.35 | 6.55 x 6.55 x 1.00 |
| **High C** | 7.50 x 4.00 x 0.35<br>9.20 x 4.70 x 0.35 | 4.50 x 2.25 x 0.35<br>4.50 x 2.45 x 0.35 | 5.70 x 2.40 x 0.35<br>5.70 x 2.40 x 0.35 | 7.00 x 7.00 x 1.05 |

## 7. EVALUATION OF STRUCTURAL DAMAGE

The evaluation of structural damage is based on the probability of a certain bridge damage state –Almost no damage, Slight damage, Moderate damage, Extensive damage and Complete damage– after a seismic event. The probability of exceeding a specific damage state is associated to the peak ground acceleration (PGA) by means of fragility curves, Barrau (2006). They have the form of two-parameter log-normal distribution functions. The probability of exceeding a damage state $j$, $F_j$, is:

$$F_j = \Phi\left[\frac{\ln\left(a_i / c_j\right)}{\varsigma_j}\right] \tag{7.1}$$

Where $\Phi$ is the standard-normal distribution function, $c$j and $\varsigma$j are the median and log-standard deviation of the fragility curves and $a_i$ is the peak ground acceleration. Assuming that the log-standard deviation is the same in all fragility curves, the probability of a certain damage state (PDS) after the earthquake is obtained as:

$$P_{i1} = P(a_i, E_i) = 1 - F_1\left(a_i, c_1, \varsigma\right) \tag{7.2}$$

$$P_{i2} = P(a_i, E_2) = F_1\left(a_i, c_1, \varsigma\right) - F_2\left(a_i, c_2, \varsigma\right) \tag{7.3}$$

$$P_{i3} = P(a_i, E_3) = F_2\left(a_i, c_2, \varsigma\right) - F_3\left(a_i, c_3, \varsigma\right) \tag{7.4}$$

$$P_{i4} = P(a_i, E_4) = F_3\left(a_i, c_3, \varsigma\right) - F_4\left(a_i, c_4, \varsigma\right) \tag{7.5}$$

$$P_{i5} = P(a_i, E_5) = F_4\left(a_i, c_4, \varsigma\right) - F_5\left(a_i, c_5, \varsigma\right) \tag{7.6}$$

where: $P_{ij}$ is the probability of a damage state $j$ when the structure is subjected to a peak ground acceleration $a_i$.

Table 7.1 Probability of a certain damage state depending on PGA

| **PGA** | **0,2080** | **0,2392** | **0,2912** | **0,3120** | **0,3588** | **0,4368** | **0,4680** | **0,5382** | **0,6552** |
|---|---|---|---|---|---|---|---|---|---|
| **Case** | Low A | Low C | Low E | Med A | Med C | Med E | High A | High C | High E |
| **Almost no damage** | 0,7349 | 0,6852 | 0,6092 | 0,5814 | 0,5238 | 0,4423 | 0,4141 | 0,3585 | 0,2852 |
| **Slight damage** | 0,0475 | 0,0521 | 0,0572 | 0,0585 | 0,0603 | 0,0607 | 0,0603 | 0,0584 | 0,0540 |
| **Moderate damage** | 0,0999 | 0,1139 | 0,1322 | 0,1379 | 0,1479 | 0,1576 | 0,1595 | 0,1610 | 0,1575 |
| **Extensive damage** | 0,0480 | 0,0576 | 0,0718 | 0,0768 | 0,0867 | 0,0992 | 0,1030 | 0,1094 | 0,1148 |
| **Complete collapse** | 0,0488 | 0,0620 | 0,0838 | 0,0922 | 0,1103 | 0,1371 | 0,1465 | 0,1651 | 0,1885 |

Once the PDS is determined, an estimate of the damage cost is made. A Central Damage Ratio (CDR) is defined for each damage state, referring to the replacement cost of the damaged members. A Mean Damage Ratio (MDR) by means of a weighted average of the CDR with the probability PDS is defined as:

$$MDR_j = \sum\left(PDS_{ij} \cdot CDR_i\right) \tag{7.7}$$

where: $j$ refers to PGA and $i$ refers to a damage state.

Table 7.2 Mean Damage Ratio (MDR) associated to Peak Ground Acceleration (PGA)

| **Case** | **PGA** | **MDR** |
|---|---|---|
| **Low A** | 0,2080 | 9,14% |
| **Low B** | 0,2392 | 11,16% |
| **Low C** | 0,2912 | 14,33% |
| **Medium A** | 0,3120 | 15,51% |
| **Medium B** | 0,3588 | 17,97% |
| **Medium C** | 0,4368 | 21,39% |
| **High A** | 0,4680 | 22,54% |
| **High B** | 0,5382 | 24,71% |
| **High C** | 0,6552 | 27,22% |

Finally, the Damage Cost (DC) is found as follows:

$$DC_j = MDR_j \cdot RPV \tag{7.8}$$

where: $j$ refers to PGA and RPV is the replacement cost of the damaged members, including demolition.

## 8. ECONOMIC ANALYSIS

The deck and piers construction costs are calculated from the obtained cross sections. The amount of reinforcing steel is calculated assuming a fixed volumetric steel ratio. Finally, costs per cubic metre of concrete, including manpower and indirect costs, are applied to the total volume of the member to find its construction costs. For the SSB configuration, the cost of the deck is calculated using a linear per metre cost of precast I-girder. The cost of the lead rubber bearings is calculated with a linear interpolation between the cost of the largest and smallest bearings. Maintenance costs only include the replacement of lead rubber bearings in the LRB type bridge at 30, 50 and 80 years following construction. Repair costs include the repair of damaged members (piers) after the one-in-50-year earthquake. All the costs are updated to the year of construction assuming a 5% cost of capital of and 3.4% inflation. Normalization is made with the cost of CBG outside a seismic zone.

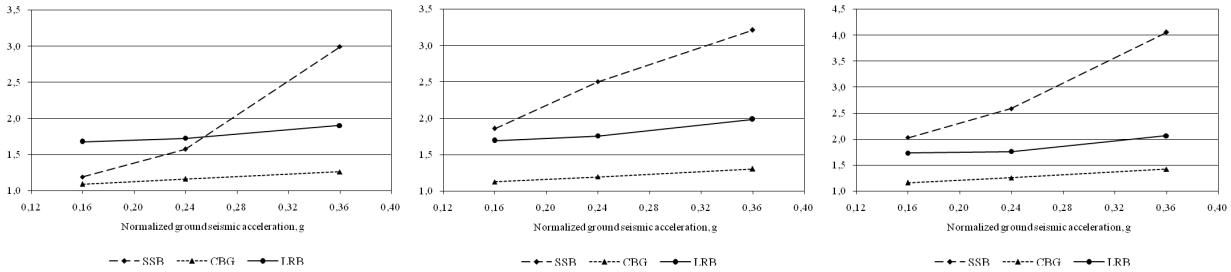


Figure 4 Bridge cost ratio depending on earthquake intensity. Ground type A, C and D, respectively. Base cost ratio equal to 1.0 refers to cost of CBG outside seismic zone.

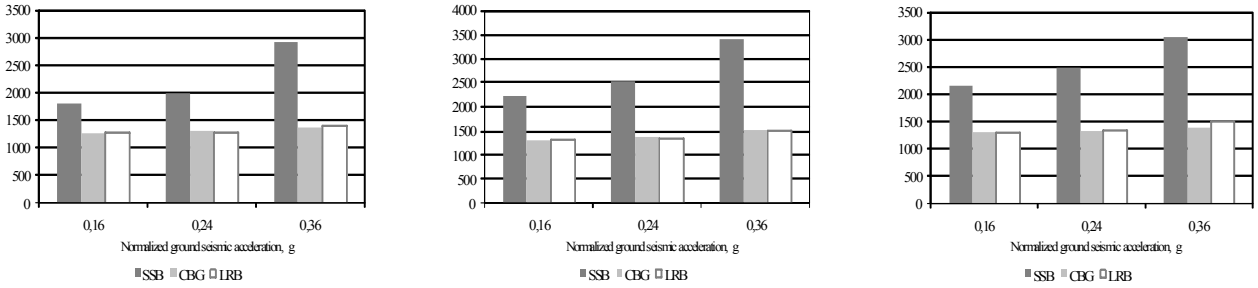


Figure 5 Total amount of concrete ($m^3$) depending on earthquake intensity. Ground type A, C and E, respectively

## REFERENCES

prEN 1998-1. Eurocode 8: Design of structures for earthquake resistance. (1998)

Georgakis C T, Mackenzie D K. (2002). Comparison of Seismic Design Methods for Irregular RC Bridges. *Proceeding of the Institution of Civil Engineers – Structures and Buildings*. **152: 2**. 167-172

SOLVIA03. (2006). Solvia Finite Element System, Solvia Engineering. Vasteras, Sweden. www.solvia.com

Barrau X. (2006). Seismic Performance of Base-Isolated Railway Bridges. *MSc Thesis*, Technical University of Denmark. pp 102